Efficient Implementation of Filter Bank Multicarrier Systems Using Circular Fast Convolution

Sohail Taheri, Mir Ghoraishi, Pei Xiao, and Lei Zhang

***Abstract*—In this paper, filter bank based multicarrier systems using fast convolution approach are investigated. We show that exploiting offset quadrature amplitude modulation enables us to perform FFT/IFFT based convolution without overlapped processing and the circular distortion can be discarded as a part of orthogonal interference terms. This property has two advantages. Firstly, it leads to spectral efficiency enhancement in the system by removing the prototype filter transients. Secondly, the complexity of the system is significantly reduced due to using efficient FFT algorithms for convolution. The new scheme is compared with the conventional waveforms in terms of out of band radiation, orthogonality, spectral efficiency and complexity. The performance of the receiver and the equalization methods are investigated and compared with other waveforms through simulations. Moreover, based on the time variant nature of the filter response of the proposed scheme, a pilot based channel estimation technique with controlled transmit power is developed and analysed through lower bound derivations. The proposed transceiver is shown to be a competitive solution for future wireless networks.**

***Index Terms*—channel estimation, circular convolution, equalization, fast convolution, filter bank, multicarrier systems, wireless communication**

I. Introduction

Dramatic growth in mobile data communication necessitates the development of wireless networks to address the new challenges in spectrum use scenarios such as cognitive radio and opportunistic dynamic radio access in an efficient and flexible way. Toward this end, it is desirable to aggregate multiple non-contiguous chunks of spectrum to achieve high data rates. Thus, highly flexible waveforms are required to effectively allocate the demanding spectrum to the users, providing rapidly decaying transition bands and high out-of-band (OoB) attenuation for synchronization immunity and avoiding interference between users. Multicarrier modulation (MCM) with its appealing characteristics such as simpler equalization and adaptive modulation techniques, presents the key element in efficient spectrum usage by activating the subcarriers in the available frequency slots.

Currently, orthogonal frequency division multiplexing (OFDM) is the dominating MCM technique and has been widely deployed in practical systems. Although channel equalization is simplified by using cyclic prefix (CP) and extension to the multiple antenna scenario is relatively straightforward, it suffers from poor OoB radiation, causing interference with the adjacent bands, and posing strict orthogonality requirements. In a system with synchronization non-idealities, a waveform with good localization in frequency, can provide more robustness against carrier frequency errors [1]. Therefore, OFDM is not the practical option for future wireless communications.

In order to address the drawbacks inherent in OFDM systems, filter bank multicarrier (FBMC) with offset quadrature amplitude modulation (OQAM) was proposed [2]–[6]. The main advantage of FBMC/OQAM over OFDM is that the non-adjacent subchannels are separated using well-localized filters in frequency domain, to reduce inter carrier interference and OoB radiations. Thus, the aforementioned shortcomings associated with OFDM can be relaxed using FBMC/OQAM. The key idea is splitting the real and imaginary parts of the symbols, upsampling and filtering them. Consequently, orthogonality holds only in real field in FBMC systems. This is because according to Balian-Low theorem [7]–[9], there is no way to utilize a well-localized prototype filter in both time and frequency, along with maintaining orthogonality and transmitting at Nyquist rate. Thus, relaxing the orthogonality condition can guarantee the other two factors. In addition to FBMC/OQAM, there are other types of FBMC like filtered multitone, and cosine-modulated multitone [9] which are not our concern in this work. For brevity, we term FBMC/OQAM as FBMC in the following.

In spite of advantages over OFDM, there are some open issues to be solved in order to make FBMC a viable solution in practical applications. Potentially, FBMC has better spectral efficiency compared to OFDM thanks to OQAM modulation and CP removal. However, the actual efficiency decreases due to the filter transients when passing the transmit signal through the polyphase filter. Assuming an unlimited transmission block, this overhead is negligible. Nevertheless, when the transmission data is divided to shorter blocks, significant overhead incurs due to the tail effect in FBMC. Hence, the transmission might become challenging in the applications with short messages such as machine-type communications [10]. Burst truncation is an obvious solution to compensate the loss in spectral efficiency [11], [12]. It has been shown that part of the signal tails can be omitted before transmitting the FBMC signal, which is a trade-off between orthogonality and OoB attenuation performance versus spectral efficiency. However, truncating the whole tail would severely degrade the orthogonality of the edge symbols. In [13], an edge processing approach for the transmission block is proposed to extend the data transmission over the signal tails. As such, the tail inefficiency is recovered. Nevertheless, the solution has been proposed for a case where the filter is very short and there is no further discussion on longer filters. Authors in [14]

The authors are with the Institute for Communication Systems, Home of 5G Innovation Centre, University of Surrey, Guildford, GU2 7XH, United Kingdom. (email: {s.taheri, m.ghoraishi, p.xiao, lei.zhang}@surrey.ac.uk)

proposed a method of tail removal by making the transmit signal periodical in order to satisfy the circular convolution property. Similar approach has been taken by authors in [15], [16] named as windowed CP based circular OQAM (WCP/COQAM). These methods perform circular convolution over the whole block of symbols. One of the problems in WCP/COQAM systems is that the channel must be constant over the block of symbols, because the channel equalization is performed over the whole block at once. As a result, this system is heavily susceptible to channel variations throughout the block of symbols. Moreover, the complexity in this system is somewhat higher than FBMC, depending on the number of symbols in the block.

Fast convolution schemes for FBMC implementation have been studied by capitalizing on the efficient implementation of convolution using fast Fourier transform (FFT), leading to complexity reduction of the system. The two well-known fast convolution methods are *overlap-add* and *overlap-save* processing. The former has been proposed in [17], [18], named as frequency spreading FBMC (FS-FBMC), and is thoroughly analysed in [19]–[21]. Comprehensive analysis of implementing uniform and non-uniform filter banks with overlap-save processing can be found in [22], [23]. Different aspects of implementing FBMC using this method were investigated in [24]–[28]. Traditionally, the main point to be considered in fast convolution is circular distortion avoidance. That is, in filtering with FFT/IFFT operations, the length of the window should cover the length of the portion of the signal and the filter additionally. This has been taken into account in the above works.

In this paper, we exploit the circular fast convolution (CFC) scheme to tackle the aforementioned problems in FBMC and WCP/COQAM systems. The contributions of this paper can be summarized as follows:

- A mathematical model for the fast convolution scheme is developed. It is a general model with which the conventional FBMC scheme, as well as FS-FBMC and WCP/COQAM can be described.
- We will show that the distortion due to circular convolution in OQAM signals is orthogonal to the main body of the signal and can be easily discarded at the receiver side. As a result of this property, no transient signal is generated during the signal modulation process. Moreover, significant complexity reduction in modulation and demodulation process is achieved using CFC-FBMC scheme, which is of vital importance for the multi-streaming case.
- Pilot-based channel estimation for FBMC has always been challenging due to contamination of the pilots by the interference from their adjacent data symbols [29]–[36]. Taking the time-variant transmultiplexer response of the CFC-FBMC system into account, a precoding scheme with controlled transmit power for pilot-based channel estimation, dedicated to CFC-FBMC, is developed and evaluated against the Cramér-Rao lower bound. This technique enables us to employ the complex pilots at the receiver side without the unknown interference.
- CFC-FBMC scheme with the high resolution equalization property enables the system to operate in highly dispersive environments. In the meantime, the proposed scheme inherits all the advantages of FBMC.

The rest of this paper is organized as follows. In Sec. II the system model of the standard FBMC is reviewed. Then, a model is provided for fast convolution representation of FBMC. The effect of circular convolution and orthogonality of circular distortion on the demodulated received signal is investigated in Sec. III and based on this, the circular fast convolution based FBMC system (CFC-FBMC) is proposed. Meanwhile, orthogonality, OoB radiations, and spectral efficiency are analysed. Sec. IV is dedicated to receiver processing of the proposed system in the presence of dispersive multipath channels. High and low resolution equalization schemes are discussed and a pilot based channel estimation scheme is proposed. Complexity of the transmitter and the receiver of the proposed system is calculated and compared with standard FBMC and OFDM systems in Sec. V. Finally, the system performance analysis and comparisons through simulations are provided in Sec. VI.

Notations: $[a]_b$ denotes $\mod(a,b)$ operation. $\langle a,b\rangle$ is the projection of a on b and $(*)$ is complex conjugate operation. $\circledast$ and $\odot$ are linear and circular convolution respectively. $\mathrm{E}[.]$ denotes expectation value. $\uparrow a$ and $\downarrow a$ are upsampling and downsampling processes with the factor of a. $\Re\{.\}$ and $\Im\{.\}$ are real part and imaginary part operations, respectively. And $\delta[n]$ is the Kronecker delta function. $\mathbb{C}$ and $\mathbb{R}$ denote the set of complex and real numbers respectively.

II. FBMC System Model

In this section, the standard structure of the FBMC system with synthesis-analysis filter bank or transmultiplexer (TMUX) structure is reviewed. Then, fast convolution representation of the system is developed.

A. Standard Structure

The TMUX structure of the FBMC system is depicted in Fig. 1 [37]. The main blocks are OQAM pre-processing, synthesis filter bank (SFB), analysis filter bank (AFB), and OQAM post-processing. As we focus on SFB and AFB blocks in this section, it is assumed that the transmission channel is ideal, i.e. the transmitter and receiver blocks are connected directly for simplicity.

In OQAM pre-processing ($\mathbb{C}2\mathbb{R}$) blocks, the input complex symbols $c_{m,n}$ are converted to real symbols, where $m = 0,1,\ldots,M-1$ and *n = 0,1,…,N-1* are subcarrier index and symbol index respectively. Real and imaginary parts of $c_{m,n}$ are upsampled by a factor of 2 so that

$$c^R_{m,n} = \begin{cases} \Re\{c_{m,\frac{n}{2}}\} & n \text{ even} \\ 0 & \text{elsewhere,} \end{cases} \tag{1}$$

and

$$c^I_{m,n} = \begin{cases} \Im\{c_{m,\frac{n}{2}}\} & n \text{ even} \\ 0 & \text{elsewhere.} \end{cases} \tag{2}$$

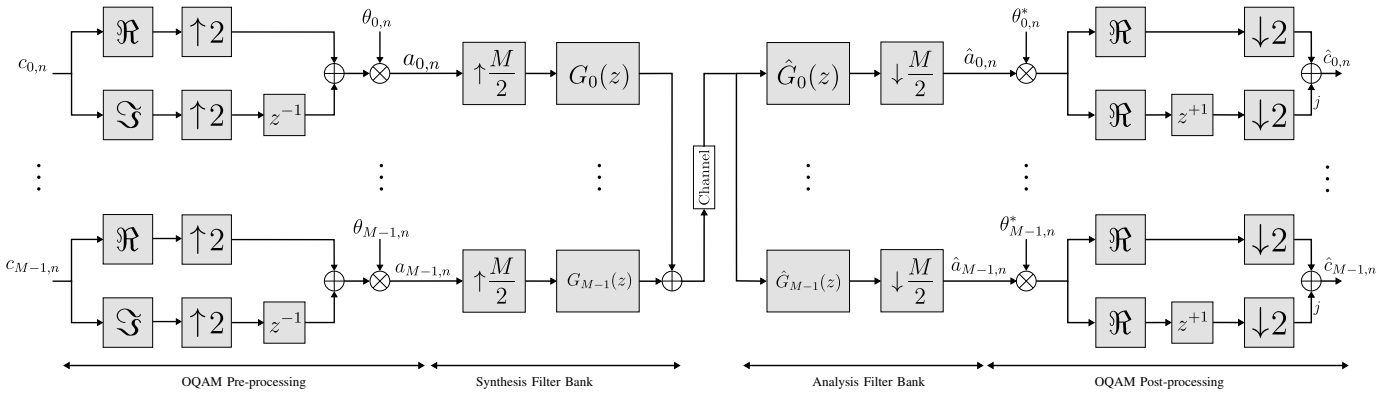

Fig. 1. Direct form representation of FBMC transceiver model

Then, $c^I_{m,n}$ is staggered by one unit and is combined with the real part samples to complete OQAM pre-processing as

$$a_{m,n} = \theta_{m,n}\{c^R_{m,n} + c^I_{m,n-1}\} = a^R_{m,n} + a^I_{m,n}, \quad (3)$$

wherein *n = 0,1,…,2N-1* and

$$\theta_{m,n} = e^{j\frac{\pi}{2}(m+n)} = j^{(m+n)}. \quad (4)$$

In the SFB block, the signals $a_{m,n}$ are upsampled by $M/2$ and filtered with their corresponding filter $g_m[k]$ to form M subchannels. The transmitted signal $s[k]$ is the sum of the filtered subchannels and can be written as [38]

$$s[k] = \sum_{n=-\infty}^{+\infty} \sum_{m=0}^{M-1} a_{m,n} g_m[k - nM/2], \quad (5)$$

where

$$g_m[k] = e^{j\frac{2\pi}{M}mk} g[k], \quad (6)$$

which represents a class of complex modulated filter banks, and $g[k]$ is a real-valued low-pass filter with the length $L_g = PM$. P is an integer number which indicates the overlap factor of the filter.

In the AFB block, the demodulated signal $\hat{a}_{m,n}$ can be extracted by projection of the received signal $r[k]$ on the corresponding receive subchannel filter $\hat{g}_m[k]$ as

$$\hat{a}_{m,n} = \langle r[k], \hat{g}_m[k] \rangle \triangleq \sum_{k=-\infty}^{+\infty} r[k]\hat{g}_m[k - nM/2], \quad (7)$$

where,

$$\hat{g}_m[k] = g^*_m[k] = e^{-j\frac{2\pi}{M}mk} g[k]. \quad (8)$$

The signal $\hat{a}_{m,n}$ carries the transmitted OQAM symbols $a_{m,n}$ and additional interference terms as

$$\hat{a}_{m,n} = a_{m,n} + u_{m,n}, \quad (9)$$

where $u_{m,n}$, known as *intrinsic interference*, is in quadrature with $a_{m,n}$ and is defined as

$$u_{m,n} = \sum_{(\bar{m},\bar{n})\neq(m,n)} a_{\bar{m},\bar{n}} \underbrace{g_{\bar{m}}[k - \bar{n}M/2]\hat{g}_m[k - nM/2]}_{\langle p \rangle^{m,n}_{\bar{m},\bar{n}}}, \quad (10)$$

where $\langle p \rangle^{m,n}_{\bar{m},\bar{n}}$ is the TMUX response of the system which depends on the employed prototype filter. Finally, retrieving the complex symbols $\hat{c}_{m,n}$ from $\hat{a}_{m,n}$ in the OQAM post-processing ($\mathbb{R}2\mathbb{C}$) block is straightforward as in Fig. 1.

B. Fast Convolution Representation of FBMC

Frequency domain filtering uses the principle of *multiplication* in the frequency domain corresponding to *convolution* in the time domain. In real-time applications such as communication systems, the long sequences are segmented into smaller blocks. The segments are transformed to frequency domain using FFT, multiplied by the prototype filter, and then transformed to the time domain again by IFFT operation. The advantage of using FFT is that it makes the convolution more efficient and faster. Therefore, this approach is also known as *fast convolution* [22]. The problem of using fast convolution is the cyclic convolution property of FFT which causes cyclic distortion. In order to perform a linear convolution, this cyclic distortion must be avoided [39].

There are two well-known approaches to generate a signal without cyclic distortions named as overlap-add and overlap-save processing methods. Assuming a single carrier signal $a[k]$ is segmented to smaller blocks with the length of L_a. the length of the FFT windows should be $L = L_a + L_p - 1$, where L_p is the filter length. With the overlap-add processing, the segments are zero-padded to reach the size L. The signals $\hat{a}_l[k]$ are the filtered versions of the zero-padded segments. In order to form the final signal $\hat{a}[k]$, the segment $\hat{a}_l[k]$ is overlapped with and added to its adjacent segments, i.e., $\hat{a}[k] = \sum \hat{a}_l[k - lL_a]$. In overlap-save processing, instead of window extension with zeros, the signal is segmented to overlapped blocks. The final signal is obtained by discarding the overlapped parts of the filtered segments and concatenating them. Therefore, this method is also called *overlap-discard*.

In order to represent FBMC with fast convolution scheme, it would be better to start with frequency-domain representation of the set of SFB and AFB filters. It is assumed that the employed prototype filter $g[k]$ has a frequency sampling based design approach as in [37], [40]–[42]. Using this approach, a number of FFT bins of the prototype filter, including passband and transition bands are non-zero, while the stopband weights are approximately zero [43]. The FFT output of $g[k]$ over the window size $LM/2$ contains $L - 1$ real-valued non-zero taps. Using (6) and denoting $K = L/2$, the FFT of the SFB filters

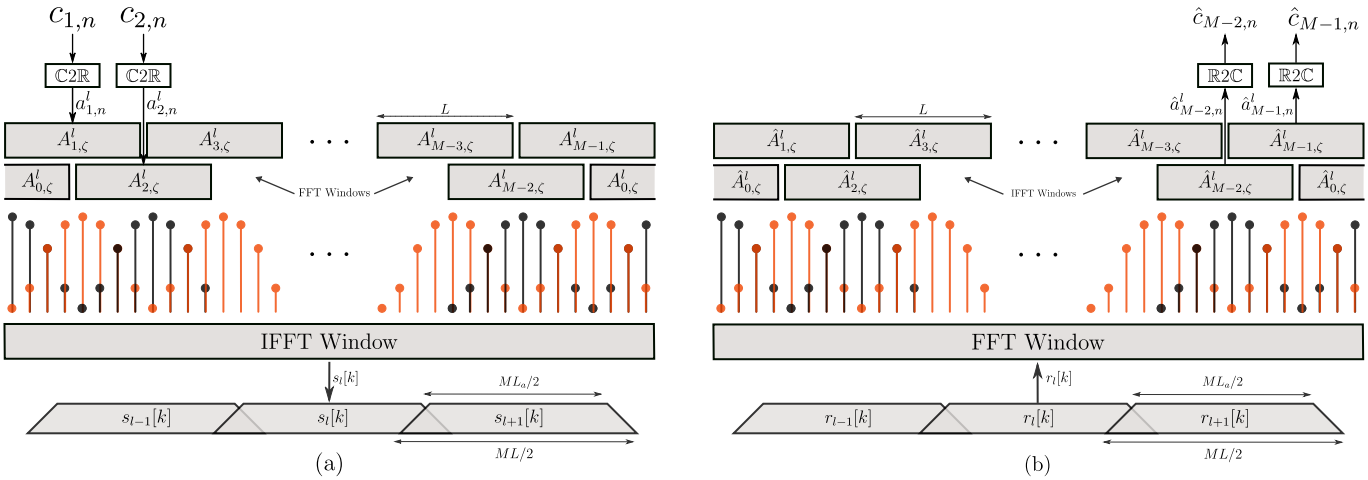

Fig. 2. FBMC systems using fast convolution scheme with $L = 8$. Filtering per subchannel is performed in frequency domain and the final transmit signal is formed using the overlap-add method

over the window KM can be derived as

$$\begin{aligned} G_m[\zeta] &= \sum_{k=0}^{KM-1} g[k] e^{j\frac{2\pi}{M}mk} e^{-j\frac{2\pi}{KM}\zeta k} \\ &= \sum_{k=0}^{KM-1} g[k] e^{-j\frac{2\pi}{KM}(\zeta - mK)k}. \end{aligned} \tag{11}$$

The parameter K should be chosen so that $K = P$ or to be an integer multiple of P to cover L_g. It is clear that the frequency response of the mth SFB filter is the circularly shifted version of $G_0[\zeta]$ by mK taps, i.e. $G_m[\zeta] = G_0[\zeta - mK]_{KM}$. Fig. 2 shows the frequency response of the SFB filters with $L-1$ non-zero taps as well as the L-sized subchannels where the distance between two adjacent subchannels is K. Accordingly, the combination of the M subchannels with L taps form an IFFT window with the length KM.

In order to perform overlap-add processing, the signal $a_{m,n}$ is segmented along symbol index axis as a_{m,lL_a+n} where $n = 0, 1, \ldots, L_a - 1$. The transformed version of the zero-padded l^{th} segment of a_{m,lL_a+n}, i.e. $a^l_{m,n}$, becomes

$$A^l_{m,\zeta} = \sum_{n=0}^{L-1} a^l_{m,n} e^{-j\frac{2\pi}{L}n\zeta}. \tag{12}$$

Fig. 2.a illustrates the FFT windows on each subchannel. The outputs of the FFT windows are multiplied to the corresponding filter taps and then added to the IFFT window to perform a M-channel long IFFT operation. Thus, the lth segment of the transmit signal can be written as

$$s_l[k] = \sum_{\zeta=0}^{KM-1} \sum_{m=0}^{M-1} A^l_{m,[\zeta-(m-1)K]_{KM}} G_m[\zeta] e^{j\frac{2\pi}{KM}\zeta k}. \tag{13}$$

Eventually, the transmit signal is the overlapped addition of the segments as

$$s[k] = \sum_{l=-\infty}^{+\infty} s_l[k - lL_aM/2]. \tag{14}$$

The structure of the receiver is depicted in Fig. 2.b, wherein the long IFFT operation is replaced by FFT and short FFTs by IFFTs. The received signal is decomposed to overlapped segments of size KM as

$$r_l[k] = r[lML_a/2 + k], \quad k \in [0, MK - 1]. \tag{15}$$

The short IFFT inputs for each subchannel is extracted as

$$\hat{A}^l_{m,\zeta} = G^*_m[\zeta] \sum_{k=0}^{KM-1} r_l[k] e^{-j\frac{2\pi}{KM}\zeta k}, \tag{16}$$

which is non-zero at $\zeta \in [mK - K, mK + K - 1]$. The short IFFT operation on the non-zero window results in

$$\hat{a}^l_{m,n} = \sum_{\zeta=0}^{L-1} \hat{A}^l_{m,[\zeta+(m-1)K]_{KM}} e^{j\frac{2\pi}{L}n\zeta}. \tag{17}$$

Regardless of the corresponding bins which carry zero in $a^l_{m,n}$, the signal $\hat{a}_{m,n}$ can be reconstructed at the receiver by concatenating the received segments. Consequently, the transmitted complex symbols can be recovered through the OQAM post-processing block.

In the frequency spreading FBMC scheme developed in [17], [18], [20], the system with $L = 8$ and $L_a = 1$, performs overlap-add processing to generate the FBMC waveform.

III. Circular Fast Convolution Based FBMC Scheme (CFC-FBMC)

So far, we have introduced the conventional convolution methods to generate FBMC signal. Generally in FBMC systems, localization of frequency leads to not-so-good time localization [12]. That is, the length of the impulse response of the prototype filter typically exceeds the symbol duration. As a result, modulation of a block of symbols in FBMC, incurs relatively long tails on both sides of the block. Assuming N QAM symbols to be transmitted, the number of generated samples is $M(N+P-1/2)$, where the $M(P-1/2)$ overhead samples degrade the spectral efficiency of the system. Tail truncation can compensate the loss in spectral efficiency.

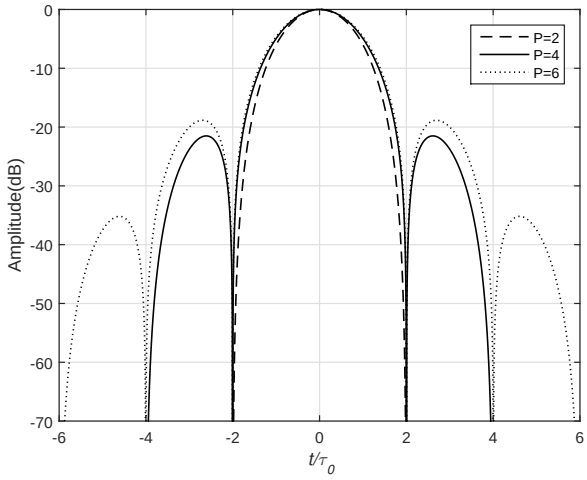

Fig. 3. Energy distribution of correlation of PHYDYAS transmit and receive filter for *P*=2,4,6 in time domain

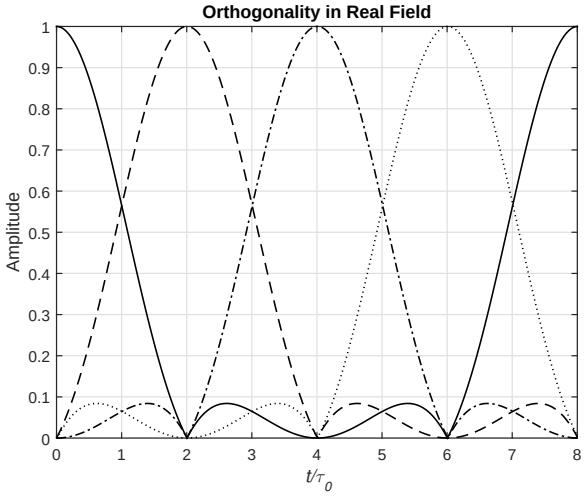

Fig. 4. $2n\tau_0$ circularly shifting of $p(t)$ guarantees orthogonality in real field

However, it distorts the symbols at the edges of the block and is not able to solve the problem completely.

In this section, the potential effect of circular convolution over each subchannel in frequency domain processing of FBMC is considered to address the aforementioned problem. It is assumed that the transmission channel is ideal. Non-ideal channels are addressed in Sec. IV.

As previously mentioned, the OQAM symbols $a_{m,n}$ in (3) comprise staggered real and imaginary part of the QAM symbols, which allow the system to exploit localized filters in time and frequency. The duration of OQAM symbols is $\tau_0 = T/2 = MT_s/2$, where T and T_s are QAM symbol duration and sampling interval respectively.

In order to obtain orthogonality in the real field, the correlation of the transmit and receive filters must be zero in time at the multiples of $2\tau_0$ [9]. Let us define the continuous-time correlation of the transmit and receive filters as $p(t) = g(t) \circledast g(-t)$. Fig. 3 shows the energy distribution of $p(t)$ for PHYDYAS filter [40]–[42] in time domain for three values of P. The well-localized filters in time domain, contain zeros at $t = \pm 2\tau_0, \pm 4\tau_0, \cdots$. $p[n]$ is defined as the sampled version of $p(t)$ in Fig. 3 at $t = n\tau_0$, where its length is L_p.

Theorem. *It is assumed that the OQAM signal $a_{m,n}$ is segmented to L-sized portions as $a^l_{m,n} = a_{m,lL+n}$ where $n = 0, 1, \ldots, L-1$ and L is even. The circular convolution operation between $a^l_{m,n}$ and $p[n]$ over a L-sized window results in a filtered signal where its circular distortion is in quadrature with the desired signal $a^l_{m,n}$.*

Proof. We start with the subchannel filtering process of the signal $\Re\{a_{m,n}\} = a^R_{m,n}$ over the lth segment. For simplicity, the subchannel index *m* is dropped and $a^R_{m,n}$ is shown as $a^R[n]$ because of the same calculations for all of the subchannels. The signal $a^R[n]$ with zeros at its odd indexes and over a window of length L can be written as

$$a^R[n] = \sum_{\eta=0}^{L-1} a^R[\eta]\delta[n-\eta] = \sum_{\eta=0}^{L/2-1} a^R[2\eta]\delta[n-2\eta]. \quad (18)$$

On the other hand, as shown in Fig. 4, the circularly shifted version of $p[n]$ over the window L has the following properties

$$p[n-\eta]_L = \begin{cases} 1 & n-\eta = 0 \\ 0 & n-\eta = 2\bar{n}, \bar{n} \neq 0. \end{cases} \quad (19)$$

Then, the circular filtering of $a^R[n]$ can be written as,

$$\hat{a}^R[n] = \sum_{\eta=0}^{L-1} a^R[\eta]p[n-\eta]_L = \sum_{\eta=0}^{L/2-1} a^R[2\eta]p[n-2\eta]_L. \quad (20)$$

From (19) and (20), it is clear that $\hat{a}^R[n] = a^R[n]$ for $n = 0, 2, \ldots, L-2$. Hence, (20) can be written as

$$\hat{a}^R[n] = \sum_{\eta=0}^{L/2-1} a^R[2\eta]\delta[n-2\eta] + u^R_c[2\eta+1]\delta[n-(2\eta+1)], \quad (21)$$

where $u^R_c[n]$ contains the circular distortion of the convolution, which is orthogonal to $a^R[n]$ and accompanies the signal $\Im\{a_{m,n}\} = a^I_{m,n}$ as a part of intrinsic interference at the receiver. That is, although circular convolution is performed over the window $L_a = L$, near perfect reconstruction (NPR) can be achieved at the receiver.

Same happens when $a^I_{m,n}$, with data on odd indexes, is circularly convolved with $p[n]$. Regardless of the subchannel index, $a^I[n]$ can be written as

$$a^I[n] = \sum_{\eta=0}^{L/2-1} a^I[2\eta+1]\delta[n-(2\eta+1)]. \quad (22)$$

Then, circular filtering of $a^I[n]$ yields

$$\begin{aligned} \hat{a}^I[n] &= \sum_{\eta=0}^{L/2-1} a^I[2\eta+1]p[n-(2\eta+1)]_L \\ &= \sum_{\eta=0}^{L/2-1} a^I[2\eta+1]\delta[n-(2\eta+1)] + u^I_c[2\eta]\delta[n-2\eta] \end{aligned} \quad (23)$$

where $u_c^I[n]$ is an orthogonal signal to $a^I[n]$ and accompanies the signal $a_{m,n}^R$ as a part of intrinsic interference.

According to (3), it is clear that $a^R[n]$ is a pure real signal, while $a^I[n]$ is pure imaginary. Consequently, the addition of the signals, $\hat{a}[n] = \hat{a}^R[n] + \hat{a}^I[n]$ results in a filtered signal wherein the transmitted real symbols can be easily recovered. □

The idea is extended to multiple subchannels to generate FBMC signal in frequency domain as in Fig. 2. The convolution on each subchannel is performed by *L*-sized FFT and IFFT operations, while the OQAM symbols $a_{m,n}$ are segmented with the size $L = L_a$, i.e. $a_{m,lL+n}$, without any concern about the circular distortion.

In order to reach the maximum spectral efficiency, the number of QAM symbols in a block should be chosen so that $N = N'L/2$, where N' is an arbitrary integer number. Hence, $N'L$ generated OQAM symbols can utilize all the capacity of the segments and no extra tail is generated. Proper choice of the prototype filter and the window length L, provides flexibility to cover a wide range of N with the highest spectral efficiency. The limiting condition for choosing L is $L \geq L_p$ which means that the subchannel window must cover the length of $p[n]$. Moreover, it must be even, as the length of $a_{m,n}$ in time is $2N$. Then, the lth segment of transmit multicarrier signal $s_l[k]$ is generated using (13) and (14).

CP Insertion and Windowing: As the circular convolution forces a rectangular window to the segments [44], sharp edges of the transmit signal segments and discontinuity between them, causes degradation of OoB radiation. On the other hand, inter segment interference in multipath channels degrades the performance of the system. The mentioned problems necessitates CP insertion between segments as well as windowing.

The segments $s_l[k]$ can be treated as long symbols with the sampling rate $f_s = MF$, where F is the subchannel spacing. Accordingly, a CP can be added to the segments to increase their robustness against multipath channels.

In order to improve the OoB attenuation performance, the edges can be smoothed through a simple windowing process. To do so, a window using Hamming coefficients $w[k] = 0.54 - 0.46\cos\big(\pi k/(L_w - 1)\big)$ is defined so that

$$\bar{w}[k] = \begin{cases} w[k + L_{CP} + L_w] & -(L_{CP}+L_w) \leq k \leq -L_{CP}-1 \\ 1 & -L_{CP} \leq k \leq KM-1 \\ w[-k + KM + L_w - 1] & KM \leq k \leq KM+L_w-1, \end{cases} \tag{24}$$

where L_{CP} and L_w are the CP length and the window length respectively. Hence, the lth windowed and CP-added segment is represented as $\bar{s}_l[k] = s_l[k]_{MK}\bar{w}[k]$ where $k \in [-(L_{CP} + L_w), MK + L_w - 1]$. The windowed parts of the adjacent segments can overlap. Thus, the final transmit signal is obtained by concatenating the segments as

$$s[k] = \sum_{l=0}^{N'-1} \bar{s}_l[k - l(MK + L_{CP})]. \tag{25}$$

More discussions on the spectral efficiency analysis and OoB radiation will be provided in this section.

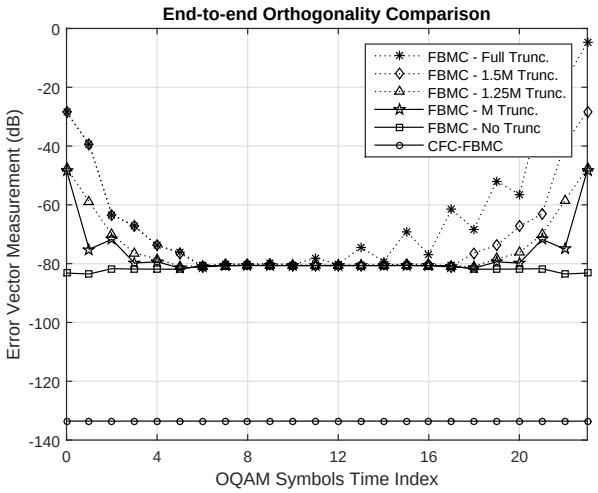

Fig. 5. Orthogonality comparison of CFC-FBMC vs. conventional FBMC with tail truncation

Demodulation: The receiver processing, assuming perfect synchronization, starts with segmenting the received signal and CP removal as

$$r_l[k] = r[l(MK + L_{CP}) + k], \quad k \in [0, MK - 1]. \tag{26}$$

The output of the subchannel IFFT operations on the lth segment carry the following information,

$$\hat{a}_{m,n}^l = a_{m,n}^l + u_{m,n}^c, \tag{27}$$

where $u_{m,n}^c$ contains different information compared to $u_{m,n}$ defined in (10) and is represented as

$$u_{m,n}^c = \sum_{(\bar{m},\bar{n}) \neq (m,n)} a_{\bar{m},[\bar{n}]_L}^l \langle p \rangle_{\bar{m},[\bar{n}]_L}^{m,n}, \quad n, \bar{n} \in [0, L-1]. \tag{28}$$

In the rest of the paper, the filter employed for analysis and simulations of FBMC, CFC-FBMC, and WCP/COQAM is PHYDYAS with $P = 4$, unless stated otherwise. The length of segments L can be 8, 12, or 16 for the filter. Choosing $L = 2K = 8$, and $N = 16$, the total number of segments are $N' = N/K = 4$, and also yields $P = K$.

A. Orthogonality Analysis

End-to-end orthogonality analysis of the transceiver in absence of channel distortion can show the quality of reconstruction in MCM systems. Here we employ error vector magnitude (EVM) on each OQAM symbol in a block to show a comparison of orthogonality between FBMC and CFC-FBMC. As mentioned earlier, FBMC suffers from tail overhead, while the problem is solved using CFC-FBMC. Thus, we can see the effect of tail truncation in the conventional FBMC as well. EVM of each OQAM symbol is defined as

$$\text{EVM}_n(\text{dB}) = 10\log_{10}\left(\frac{\sum_m |a_{m,n} - \hat{a}_{m,n}|^2}{\sum_m |a_{m,n}|^2}\right). \tag{29}$$

Fig. 5 represents orthogonality of the systems over a transmission block with $N = 12$, i.e. the number of OQAM

symbols are $2N = 24$. Comparison of EVM in CFC-FBMC and the conventional FBMC with no truncation shows that NPR is achieved by both systems. However, due to small transients at the edge of the filtered symbols which exceeds the numerical precision, orthogonality of FBMC slightly degrades [22]. These transients are not generated in CFC-FBMC.

The results for the edge symbols in FBMC are getting worse by tail truncation with amount of M, $1.25M$, and $1.5M$ samples on each side respectively. Truncation of $1.25M$ samples from each side is the optimum point between recovery of spectral efficiency and maintaining orthogonality. This is while full truncation of tails, including half of the last OQAM symbol, destroys the last two QAM symbols of the block. As a result, the length of the tail that should be kept in FBMC is M which reduces the spectral efficiency.

B. Spectral Efficiency Analysis

The general form of spectral efficiency can be defined as

$$\epsilon = \gamma(\Lambda)\alpha\beta, \tag{30}$$

where $\gamma(\Lambda)$ is the lattice density [9], α is the reduction factor due to CP insertion, and β indicates the effect of tails of the modulated block of symbols. Other parameters such as bits per symbol and coding rate are assumed to be the same for all the waveforms. The lattice density for plain OFDM and FBMC is defined as

$$\gamma(\Lambda) = \frac{1}{TF}, \tag{31}$$

which is 1 for the two systems. The parameters α and β for different waveforms have been tabulated in Table I. The range

TABLE I
SPECTRAL EFFICIENCY REDUCTION FACTORS FOR DIFFERENT WAVEFORMS

	α	β
Plain OFDM	1	1
CP-OFDM	$\frac{M}{M+L_{CP}}$	1
FBMC	1	$\frac{N}{N+P-0.5}$
FBMC-Trunc.	1	$\frac{N}{N+1}$
WCP/COQAM	$\frac{M}{M+L_{CP}/N}$	1

of spectral efficiency defined in (30) is $0 \leq \epsilon \leq 1$ where the optimum value is 1. We have shown that the tail overhead in CFC-FBMC can be minimized to achieve a critically-sampled signal like plain OFDM. While the parameter β is 1 due to tail removal, α for the system becomes

$$\alpha = \frac{M}{M + L_{CP}/K} \tag{32}$$

which shows the larger K, the closer ϵ to 1.

Fig. 6 shows spectral efficiency comparison of CFC-FBMC, and other waveforms such as CP-OFDM, conventional FBMC with truncated tails, and WCP/COQAM. The length of CP is the same as normal and extended CP in long term evolution (LTE) standard [45]. WCP/COQAM has the best spectral efficiency among the compared waveforms, although it has some drawbacks such as higher complexity and equalization

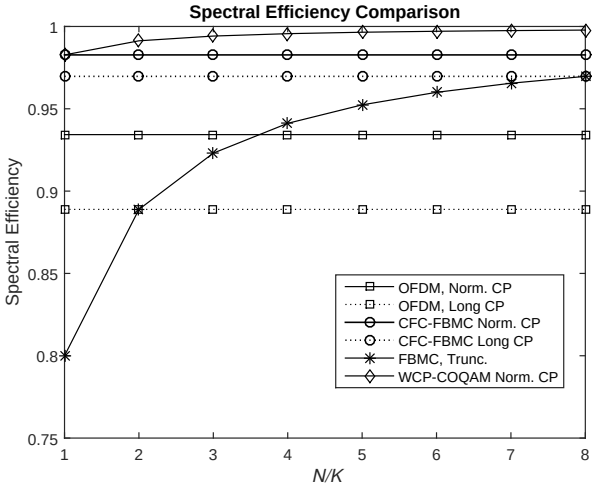

Fig. 6. Spectral efficiency comparison of different systems vs. normalized number of symbols with respect to $K = 4$

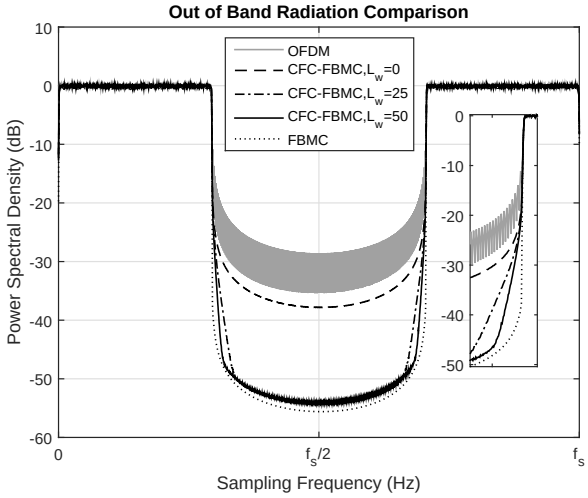

Fig. 7. PSD comparison of waveforms, $M = 512$, $L = 8$

in high mobility scenarios which will be investigated later on. CFC-FBMC outperform OFDM and FBMC for short blocks up to 32 QAM symbols. For very large blocks, truncated FBMC gradually converges to 1.

C. Out of Band Radiation Comparison

Fig. 7 represent comparison of power spectral density (PSD) of OFDM, FBMC, and CFC-FBMC with $L_w = 0, 25, 50$ samples. Although CFC-FBMC without windowing, i.e. $L_w = 0$ still has better OoB radiation performance than OFDM, its performance degrades compared to FBMC since the circular convolution leads to a rectangular window impact to the PSD of CFC-FBMC. By increasing L_w, the stop-band decay becomes as sharp as FBMC. Windowing with $L_w = 25$ provides an acceptable performance, to be able to reduce the guard bands for efficiently use of the spectrum.

IV. Receiver Processing

The CFC-FBMC scheme was presented in the previous section assuming ideal transmission channel. In this section, the receiver processes in presence of multipath channels are analysed.

The received signal after passing through the channel can be written as

$$r[k] = s[k] \circledast h[k,\eta] + \psi[k], \tag{33}$$

where $h[k,\eta]$ is the time-varying multipath channel and $\psi[k] \sim \mathcal{CN}(0,\sigma_\psi)$ is the complex additive white Gaussian noise (AWGN). After CP removal, performing the long FFT operation over the lth segment of the received signal yields

$$R[\zeta] = H_\zeta^l \sum_{m=0}^{M-1} A^l_{m,[\zeta-(m-1)K]_{KM}} G_m[\zeta] + \Psi[\zeta], \tag{34}$$

where H_ζ^l is the channel frequency response which is assumed to be static over the segment, and $\Psi[\zeta]$ is the noise term. In order to perform equalization, a high resolution (HR) equalization over the FFT output (KM taps) is required [20], i.e., each subchannel is equalized over its L taps prior to short IFFT operation. Performing zero-forcing (ZF) equalization yields

$$R_{\text{ZF}}[\zeta] = \sum_{m=0}^{M-1} A^l_{m,[\zeta-(m-1)K]_{MK}} G_m[\zeta] + \Psi[\zeta]/H_\zeta^l. \tag{35}$$

Then, the symbols on the subchannel $\hat{A}_{m,\zeta}$ can be extracted using (16), (17) and OQAM post-processing.

In case of moderate channel dispersions, the channel H_ζ^l is approximately constant over each subchannel taps. Therefore, (34) can be reformed as

$$R[\zeta] = \sum_{m=0}^{M-1} H_m^l A^l_{m,[\zeta-(m-1)K]_{MK}} G_m[\zeta] + \Psi[\zeta], \tag{36}$$

where H_m^l is the channel response over the mth subchannel. Extracting the mth subchannel, filtering, and performing short IFFT yields

$$\hat{a}_{m,n} = H_m^l (a_{m,n} + u^c_{m,n}) + \bar{\psi}_{m,n}. \tag{37}$$

Thus, the equalization can be performed as a low resolution (LR) approach where the channel information over M taps are required. The LR equalization is simpler than HR as it can be performed upon channel estimation process, but it is not optimal in highly dispersive channels. In HR equalization, the receiver has to perform two iterations, first extracting the pilots, channel estimation and interpolation over KM taps in the post IFFT stage, then moving backward to perform the equalization in the pre IFFT stage.

The noise term $\bar{\psi}_{m,n}$ in (37) is calculated as

$$\bar{\psi}_{m,n} = \sum_{\zeta=0}^{L-1} G_m^*[\zeta+(m-1)K]\Psi[\zeta+(m-1)K] e^{j\frac{2\pi}{L}n\zeta}, \tag{38}$$

which is filtered on each subchannel. It is easy to show that $\bar{\psi}_{m,n}$ follows normal distribution where its mean and variance are 0 and σ_ψ respectively, and the noise correlation between time-frequency points is $\langle p \rangle^{m,n}_{\bar{m},[\bar{n}]_L}$ [46].

A. Pilot-based Channel Estimation for CFC-FBMC

Pilot-based channel estimation is a popular method in the MCM systems to retrieve information about the transmission channel. Pilots are placed at certain time and frequency intervals. By interpolation through the rest of frequency points, the channel information over a slot of symbols is obtained. While exploitation of pilots in OFDM is straightforward, it is not a simple process in FBMC systems. As shown earlier, the pilots are contaminated with intrinsic interference coming from the adjacent subchannels and symbols. Therefore, without knowing the interference, it is impossible to obtain channel information on that point. In this section, a precoding scheme is proposed to reconstruct the defined pilots with the unit power at the receiver side, while the transmit pilot power does not exceed the unit. The proposed precoding method for FBMC in [29] suffers from increased power consumption. [30]–[33] dealt with the overhead problem by increasing complexity at the receiver side. The Techniques in [34], [35] use precoded repetitive data patterns around the pilot to cancel the intrinsic interference on it. The method in [36] relies on the repetitive adjacent pilots at the transmitter and derivatives of the received analogue signal at the receiver side.

The proposed precoding method is designed for CFC-FBMC and considers circularly convolved signals in the precoding process, but with slight modifications, it is applicable to FBMC systems as well.

First of all, a set of neighbouring points which contribute to intrinsic interference on an arbitrary point (m_0, n_0) is defined as

$$\begin{aligned} &\Omega_{m_0,n_0} = \\ &\Big\{(m,n) | m_0 - 1 \le m \le m_0 + 1, n_0 - P + 1 \le n \le n_0 + P - 1\Big\} \\ &\Omega^*_{m_0,n_0} = \Omega_{m_0,n_0} - \Big\{(m_0,n_0)\Big\}. \end{aligned} \tag{39}$$

In CFC-FBMC, due to the circular convolution in each segment, time index n is limited to $n \in [0, L-1]$. Therefore. the symbol index interval in (39) is wrapped to $[0, L-1]$. The coefficients $\langle p \rangle^{m_0,n_0}_{m,n}$ over the set Ω_{m_0,n_0} are TMUX response of the system. The value of the TMUX response out of the set $\Omega^*_{m_0,n_0}$ is approximately zero.

A complex pilot q_{m_0,n_0} in OFDM system is equivalent to two adjacent real pilots in OQAM modulation, i.e. $(q^R_{m_0,n_0}, q^I_{m_0,n_0+1})$. The intrinsic interference on the transmitted pilots, according to (28) can be written as

$$\begin{aligned} u^R_{m_0,n_0} &= \sum_{(m,n)\in\Omega^*_{m_0,n_0}} a_{m,[n]_L} \langle p \rangle^{m_0,n_0}_{m,[n]_L} \\ &= \bar{u}^R_{m_0,n_0} + q^I_{m_0,n_0+1} \langle p \rangle^{m_0,n_0}_{m_0,n_0+1} \\ u^I_{m_0,n_0+1} &= \sum_{(m,n)\in\Omega^*_{m_0,n_0+1}} a_{m,[n]_L} \langle p \rangle^{m_0,n_0+1}_{m,[n]_L} \\ &= \bar{u}^I_{m_0,n_0+1} + q^R_{m_0,n_0} \langle p \rangle^{m_0,n_0+1}_{m_0,n_0}. \end{aligned} \tag{40}$$

Hence, the combination of the received pilots yields

$$\hat{q}_{m_0,n_0} = (q^R_{m_0,n_0} + u^R_{m_0,n_0}) + (q^I_{m_0,n_0+1} + u^I_{m_0,n_0+1}), \tag{41}$$

which is obviously not equal to q_{m_0,n_0}. $q^R_{m_0,n_0}$ and $u^I_{m_0,n_0+1}$ are both purely real-valued, while $u^R_{m_0,n_0}$ and $q^I_{m_0,n_0+1}$ are

imaginary. In order to have $\hat{q}_{m_0,n_0} = q_{m_0,n_0}$, it is possible to transmit $\tilde{q}^R$ and $\tilde{q}^I$ so that

$$\begin{aligned} \tilde{q}^R_{m_0,n_0} + \tilde{u}^I_{m_0,n_0+1} &= q^R_{m_0,n_0} \\ \tilde{q}^I_{m_0,n_0+1} + \tilde{u}^R_{m_0,n_0} &= q^I_{m_0,n_0+1}. \end{aligned} \tag{42}$$

$\tilde{u}^I_{m_0,n_0+1}$ and $\tilde{u}^R_{m_0,n_0}$ can be derived using (40). Thus, the amount of $\tilde{q}^R_{m_0,n_0}$ and $\tilde{q}^I_{m_0,n_0+1}$ is calculated as

$$\begin{aligned} \tilde{q}^R_{m_0,n_0} &= \frac{q^R_{m_0,n_0} - \bar{u}^I_{m_0,n_0+1}}{1 + \langle p \rangle^{m_0,n_0+1}_{m_0,n_0}} \\ \tilde{q}^I_{m_0,n_0+1} &= \frac{q^I_{m_0,n_0+1} - \bar{u}^R_{m_0,n_0}}{1 + \langle p \rangle^{m_0,n_0}_{m_0,n_0+1}}. \end{aligned} \tag{43}$$

As a result, by transmitting $\tilde{q}^R$ and $\tilde{q}^I$ and assuming that the channel is constant over the set Ω_{m_0,n_0}, the received samples at the two points can be combined as

$$\hat{q}_{m_0,n_0} = H_{m_0,n_0} \underbrace{(q^R_{m_0,n_0} + q^I_{m_0,n_0+1})}_{q_{m_0,n_0}} + \bar{\psi}_{m_0,n_0}, \tag{44}$$

where q_{m_0,n_0} is known to the receiver and the channel information at the point (m_0, n_0) is obtained. The channel information over the rest of subchannels can be derived via interpolation. In this work, upsampling and low-pass filtering method for interpolation has been exploited. For HR Equalization, two step interpolation is required to obtain the high resolution channel information.

The performance of the channel estimator can be evaluated using the Cramér-Rao lower bound benchmark. The proposed precoding decorrelates the pilots from their adjacent time-frequency points. Thus, the likelihood function for the unbiased estimator in (44) can be written as

$$\mathfrak{p}(\hat{q}; H) = \frac{1}{(\pi\sigma_{\bar{\psi}})^2} \exp[-\frac{(\hat{q} - qH)^*(\hat{q} - qH)}{\sigma_{\bar{\psi}}}], \tag{45}$$

where σ_{ψ} is the noise power. Then, the variance of the estimator must satisfy

$$\text{var}(\hat{H}) \geq \frac{1}{-\text{E}[\frac{\partial^2 \ln\mathfrak{p}(\hat{q}; H)}{\partial H \partial H^*}]}, \tag{46}$$

where $\ln\mathfrak{p}(\hat{q}; H)$ is the log-likelihood function. The first derivation of $\ln\mathfrak{p}(\hat{q}; H)$ yields

$$\begin{aligned} \frac{\partial \ln\mathfrak{p}(\hat{q}; H)}{\partial H} &= \frac{\bar{q}^* q - q^* H^*}{\sigma_{\bar{\psi}}} \\ &= \frac{|q|^2(\bar{q}/q - H)^*}{\sigma_{\bar{\psi}}} \\ &= \frac{|q|^2}{\sigma_{\bar{\psi}}}(\bar{H} - H)^* = J(H)\big(\bar{H} - H\big)^*. \end{aligned} \tag{47}$$

Then, the second derivation of $\ln\mathfrak{p}(\hat{q}; H)$ results in

$$\frac{\partial^2 \ln\mathfrak{p}(\hat{q}; H)}{\partial H \partial H^*} = -\frac{|q|^2}{\sigma_{\bar{\psi}}} = -J(H). \tag{48}$$

Furthermore, (47) reveals that the estimator attains the bound, i.e. it is minimum variance unbiased [47]. Hence, the variance of the estimator is

$$\text{var}(\hat{H}) = 1/\text{E}[J(H)] = \frac{\sigma_{\bar{\psi}}}{\text{E}[|q|^2]}, \tag{49}$$

where $\text{E}[|q|^2]$ is the transmitted pilot power. Defining the power of the pilots in OFDM as $\text{E}[|q|^2] = \Gamma_q$, we can calculate the power of the pilots $\tilde{q}^R$ and $\tilde{q}^I$ in the proposed pilot precoding. Clearly, the power of q^R and q^I and the OQAM symbols a is $\Gamma_{q^R} = \Gamma_{q^I} = \Gamma_a = \Gamma_q/2$, as they are real or imaginary valued. Also the power of intrinsic interference terms that accompany q^R and q^I is

$$\begin{aligned} \Gamma_{u^R} = \Gamma_{u^I} &= \sum_{(m,n)\in\Omega^*_{m_0,n_0}} \Gamma_a |\langle p \rangle^{m_0,n_0}_{m,[n]_L}|^2 \\ &= \Gamma_a \underbrace{\sum_{(m,n)\in\Omega^*_{m_0,n_0}} |\langle p \rangle^{m_0,n_0}_{m,[n]_L}|^2}_{1} = \Gamma_a. \end{aligned} \tag{50}$$

From (40) and (50), the power of $\bar{u}^R$ and $\bar{u}^I$ is

$$\Gamma_{\bar{u}^R} = \Gamma_{\bar{u}^I} = \Gamma_{u^R} - \phi^2 \Gamma_{q^I} = \Gamma_q(1 - \phi^2)/2, \tag{51}$$

where $\phi = |\langle p \rangle^{m_0,n_0}_{m_0,n_0+1}| = |\langle p \rangle^{m_0,n_0+1}_{m_0,n_0}|$. As a result, using (43) and (51), the power of the precoded pilots, i.e. $\Gamma_{\tilde{q}^R}$ and $\Gamma_{\tilde{q}^I}$ becomes

$$\Gamma_{\tilde{q}^R} = \Gamma_{\tilde{q}^I} = \frac{\Gamma_q/2 + \Gamma_q/2(1 - \phi^2)}{(1 + \phi)^2} = \frac{\Gamma_q(2 - \phi^2)}{2(1 + \phi)^2}. \tag{52}$$

For the employed prototype filter in this work, the value of ϕ is $\phi \approx 0.57$. Hence $\Gamma_{\tilde{q}^R} = \Gamma_{\tilde{q}^I} \approx 0.33\Gamma_q$ in (52), which means that pilot construction at the receiver side comes with the cost of reduced transmit power in CFC-FBMC (or FBMC in general). Consequently, (52) shows that the channel estimators in OFDM and CFC-FBMC achieve different bounds. The relation between the bounds is

$$\frac{\text{var}(\hat{H})_{\text{CFC-FBMC}}}{\text{var}(\hat{H})_{\text{OFDM}}} = \frac{2(1 + \phi)^2}{2 - \phi^2} \approx 3. \tag{53}$$

The closer (53) to 1, the better performance of channel estimation in FBMC compared to OFDM. Therefore, it is theoretically shown that the pilot-based channel estimation in FBMC cannot be as good as OFDM, unless increasing the pilots transmit power as in [29].

V. Complexity Analysis

Complexity of a waveform is an important parameter of practical concern. Choosing the short window length parameter L as a power of two enables CFC-FBMC to use efficient FFT and IFFT algorithms in convolution, leading to lower complexity compared to the standard structure of FBMC. Here, the complexity of CFC-FBMC is compared with OFDM, FBMC, and WCP/COQAM.

Typically the complexity of an algorithm is measured by the number of floating point operations (FLOPS). As the definition of FLOPS varies in different processors, we only focus on the number of real multiplications in the complexity analysis. Clearly, every complex multiplication requires four real multiplications. The parameter for the most efficient FFT algorithm, i.e. split-radix [39] is expressed as

$$C_M = M(\log_2 M - 3) + 4. \tag{54}$$

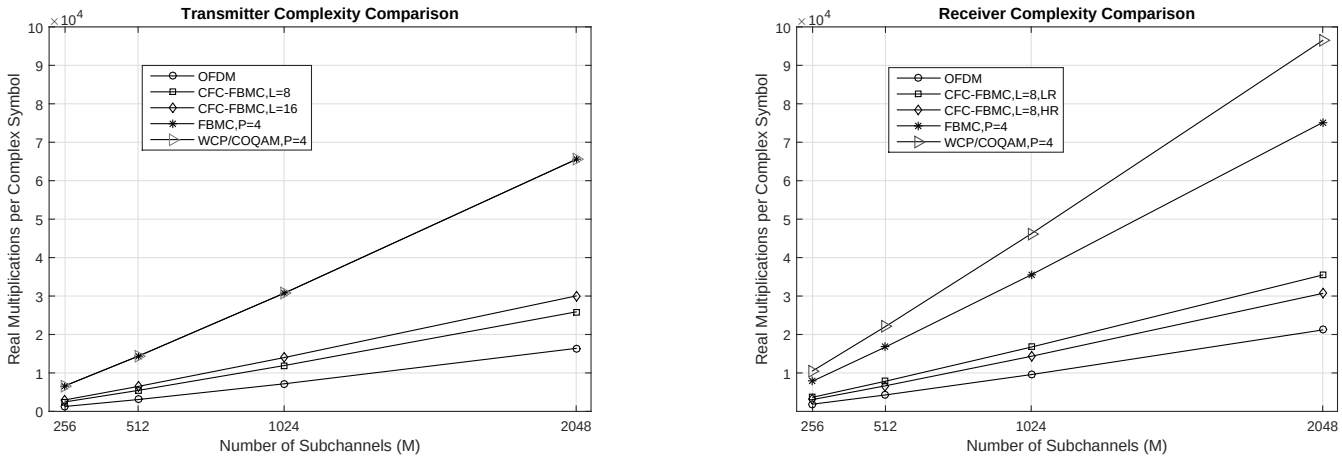

Fig. 8. Complexity comparison of transmitter and receiver processing in OFDM, FBMC, CFC-FBMC, and WCP/COQAM

a) Transmitter Processing: Every OQAM symbol in transmitter of the conventional FBMC requires an *M*-point IFFT operation with pure real or imaginary inputs, in addition to filtering with a real-valued high rate filter. Thus, the number of multiplications is

$$C'_{\text{FBMC}} = C_M + 2MP. \tag{55}$$

Consequently, the complexity of a complex symbol modulation is two times C'_{FBMC} as

$$C_{\text{FBMC}} = 2(C_M + 2MP), \tag{56}$$

while it is C_M for OFDM systms.

In CFC-FBMC, M_u active subchannels are filtered individually using short FFTs, while the filter taps are real with the first one being zero, which is not counted in calculations. Then IFFT over M subchannels with the length of MK is performed to generate the transmit signal of one segment. Each segment modulates K complex symbols, therefore, the overall multiplications for each segment is divided by K to obtain the complexity per complex symbol. It can be expressed as

$$C_{\text{CFC-FBMC}} = \frac{1}{K}\big(C_{MK} + C_L M_u + 2(L-1)M_u\big), \tag{57}$$

where C_{MK} and C_L can be obtained using (54). The complexity of WCP/COQAM transmitter is the same as FBMC, with circular shift and addition instead of linear shift.

b) Receiver Processing: In receiver processing, M_u complex multiplications for equalization process is added to the calculated complexities at the transmitter side. Hence, complexity of OFDM and FBMC systems can be summarized as follows,

$$\begin{aligned} C_{\text{OFDM}} &= C_M + 4M_u, \\ C_{\text{FBMC}} &= 2(C_M + 2MP + 4M_u), \end{aligned} \tag{58}$$

while the complexity of CFC-FBMC with LR and HR equalization is

$$\begin{aligned} C_{\text{CFC-FBMC-LR}} &= \frac{1}{K}\Big(C_{MK} + M_u\big(C_L + 2(L-1)\big) + 4LM_u\Big) \\ C_{\text{CFC-FBMC-HR}} &= \frac{1}{K}\Big(C_{MK} + M_u\big(C_L + 2(L-1)\big) + 4K(M_u+2)\Big). \end{aligned} \tag{59}$$

Fig. 8 shows the transmitter and receiver complexity comparison of OFDM, FBMC and CFC-FBMC. The minimum required window for the filter with $P = 4$ is $L = 8$. Therefore $L = 8$ and $L = 16$ has been chosen for transmitter complexity comparison. In the receiver comparison, LR and HR equalizations with $L = 8$ have been compared. Thanks to the efficient calculations, the complexity of CFC-FBMC is significantly lower than FBMC, i.e. it has been reduced to approximately half in number of real multiplications.

Complexity of WCP/COQAM receiver depends on the number of symbols in the block [16]. The complexity shown here is calculated based on the simulation parameters in the next section, i.e. $N = 16$ and $P = 4$. Hence, the length of the block samples would be a power of two and the split-radix FFT operation over the block can be performed. As it is seen, the receiver is more complex than FBMC in this scenario.

VI. Simulation Results

In this section, the performance of CFC-FBCM compared to three waveforms OFDM and FBMC and WCP/COQAM is provided through simulations. Similar to OFDM, CFC-FBMC can be used in various wireless applications such as WiFi, cellular networks, etc. In this section, we adopt a downlink scenario in which a LTE-like block with parameters summarized in Table II is used. Pilots are scattered through the block

TABLE II
Simulation Parameters

Parameters	Modulation	N	M	M_u	L	L_{CP}	L_w
Value	16-QAM	16	512	300	8	32	25

over four distributed symbols with six subchannel spacing, starting from first and fourth subchannels on each symbol Alternatively. In the simulations, perfect synchronization is assumed, i.e. there is no time and carrier frequency offset. One-tap zero forcing (ZF) equalization is performed for symbol detection. Two channels used for simulations are the extended pedestrian A (EPA), and the highly dispersive extended typical

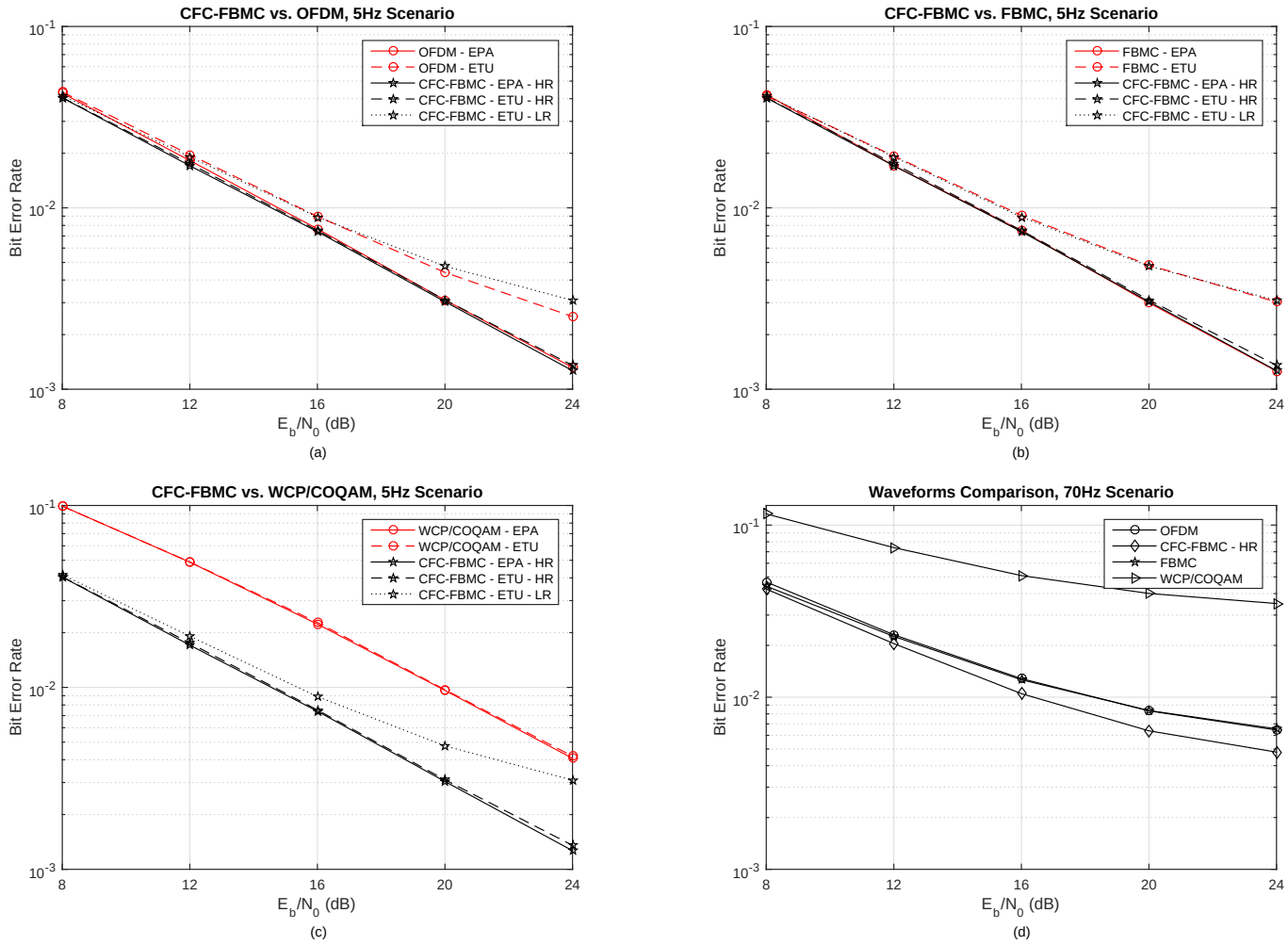

Fig. 9. Performance comparison of (a) OFDM vs. CFC-FBMC in $f_D = 5$Hz, (b) FBMC vs. CFC-FBMC in $f_D = 5$Hz, (c) WCP/COQAM vs. CFC-FBMC in $f_D = 5$Hz, and (d) all waveforms in $f_D = 70$Hz, assuming the channel information is perfectly known

urban (ETU) channel in $f_D = 5$Hz and $f_D = 70$Hz scenarios [48], where f_D is the Doppler spread.

Performance Comparison: Assuming the channel information is known, the $f_D = 5$Hz performance of OFDM and FBMC systems versus CFC-FBMC with LR and HR equalization has been compared in Fig. 9.a and 9.b respectively. Performance of OFDM, FBMC and CFC-FBMC is the same in EPA channel. In ETU channel, performance of FBMC and CFC-FBMC with LR equalization is the same, while OFDM performance is slightly better. This is mainly because in the formers, the variations of the channel frequency response over each subchannel is assumed to be constant, while variations are significant in the ETU channel. CFC-FBMC with HR equalization shows a superior performance in ETU channel which outperforms OFDM and FBMC and attains its EPA performance without degradation.

Fig. 9.c shows the comparison of WCP/COQAM and CFC-FBMC. Although the equalization of WCP/COQAM is performed in high resolution frequency domain as in CFC FBMC, the FFT operation and equalization over the whole block of symbols significantly degrades the performance even in low mobility $f_D = 5$Hz scenario wherein the channel over the symbols block is not constant. The performances of WCP/COQAM in EPA and ETU 5 Hz are the same thanks to the high resolution equalization, but it cannot compete with CFC FBMC with LR and HR equalization.

Fig. 9.d shows the performance of the four systems over double-dispersive ETU $f_D = 70$Hz scenario. While performance of CFC-FBMC is slightly better than FBMC and OFDM, WCP/COQAM fails to operate under such a harsh channel environment, due to the problem mentioned above.

Performance Comparison with Channel Estimation: In this part, channel estimation non-idealities are considered in system performances. First of all, a comparison between the proposed channel estimation for CFC-FBMC and OFDM is presented in Fig. 10 in 5 Hz Scenario. The ratio between derived lower bounds in (53) with the exploited prototype filter is approximately 3 which is shown in the figure. The resulting MSE for the systems in both channel scenarios confirm the theoretical bounds. In OFDM, the channel estimator perfectly attains the bound with a negligible degradation in ETU channel. The estimation in CFC-FBMC follows its

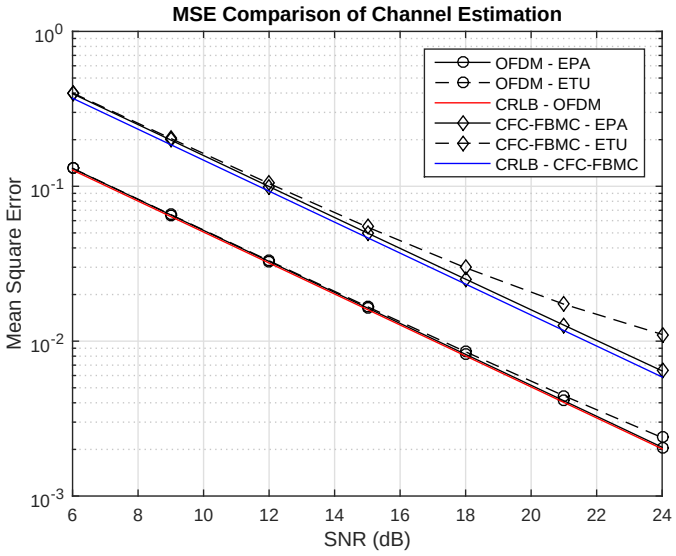

Fig. 10. MSE performance comparison of OFDM vs. CFC-FBMC, $f_D = 5$Hz Scenario

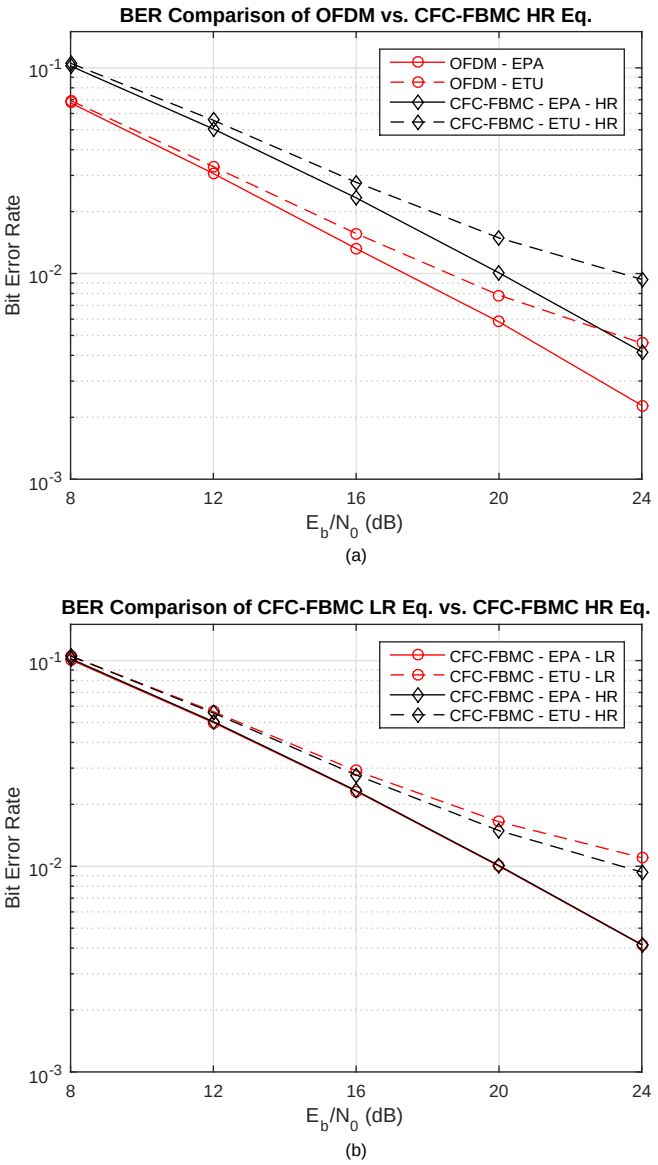

Fig. 11. BER performance comparison of OFDM vs. CFC-FBMC in presence of channel estimation, $f_D = 5$Hz Scenario

bound in EPA channel scenario, while it endures a degradation in higher SNRs in ETU channel. As the channel is not necessarily constant over adjacent subchannels, the constant channel assumption in pilot precoding is not valid. Thus the degradation in MSE performance is justified.

The impact of channel estimation is illustrated in Fig. 11. In this figure, HR equalization of CFC-FBMC is compared with OFDM and LR equalization CFC-FBMC. Comparison of Fig. 9.a and Fig. 11.a reveals that the higher MSE of channel estimator in CFC-FBMC has a negative impact on total performance of the system compared to OFDM. In the EPA scenario, there is a slight degradation, while in ETU channel, degradation is significant. Comparison of LR and HR equalization in Fig. 11.b reveals that the HR equalization performs better than LR in the ETU scenario which confirms the results with perfect channel information. However, due to the channel estimation problem in CFC-FBMC (FBMC in general), i.e. the variable channel frequency response over the set Ω_{m_0,n_0} around each pilot, HR equalization capability in the performances is not totally feasible.

Performance Comparison In The Presence of Carrier Frequency Offset (CFO): The impact of CFO on the subchannels of the waveforms is shown in Fig. 12. In this simulation, one of the subchannels is shifted in frequency domain to evaluate the signal to interference ratio (SIR) in the adjacent subchannels. As it can be seen, localization of FBMC in frequency domain enables it to minimize the interference on the subchannels, which is a pivotal advantage in separation of users in multi-user scenarios. While the performance of CFC-FBMC and WCP/COQAM is very close to FBMC, OFDM suffers from very high interference in the adjacent subchannels.

VII. Conclusion

A novel structure for filter bank based multicarrier systems has been investigated using fast convolution approach. We showed exploiting offset quadrature amplitude modulation, enables us to perform FFT/IFFT based convolution without overlapped processing while the circular distortion can be discarded as a part of orthogonal interference terms. Using such property, significant improvements was achieved in terms of spectral efficiency, orthogonality, complexity and the link-level performance compared to conventional FBMC systems. Performance of the receiver and equalization methods were investigated and compared with other waveforms thorough simulations. Moreover, based on the time variant nature of the filter response of CFC-FBMC, a pilot based channel estimation technique with controlled transmit power was proposed and analysed against lower bound derivations. The proposed transceiver was shown to be a competitive waveform processing for future wireless networks.

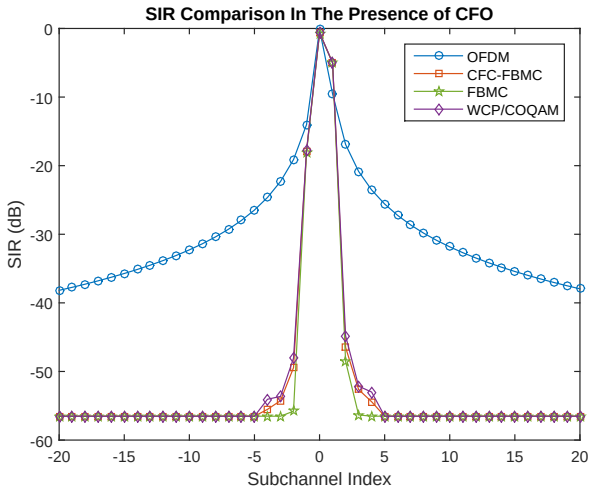

Fig. 12. Performance comparison in the presence of CFO on the center subchannel and its interference on the adjacent subchannels. $\Delta f = 0.25F$

ACKNOWLEDGMENT

This work was sponsored by the UK Engineering and Physical Sciences Research Council (EPSRC) under grant number EP/N020391/1. The authors also would like to acknowledge the support of the University of Surrey 5GIC (http://www.surrey.ac.uk/5gic) members for this work.

REFERENCES

[1] H. Saeedi-Sourck, Y. Wu, J. W. M. Bergmans, S. Sadri, and B. Farhang-Boroujeny, "Sensitivity analysis of offset QAM multicarrier systems to residual carrier frequency and timing offsets," *Signal Process.*, vol. 91, no. 7, pp. 1604–1612, Jul. 2011.

[2] B. Saltzberg, "Performance of an efficient parallel data transmission system," *IEEE Transactions on Communication Technology*, vol. 15, no. 6, pp. 805–811, December 1967.

[3] B. Farhang-Boroujeny, "OFDM versus filter bank multicarrier," *Signal Processing Magazine, IEEE*, vol. 28, no. 3, pp. 92–112, May 2011.

[4] J. Du, P. Xiao, J. Wu, and Q. Chen, "Design of isotropic orthogonal transform algorithm-based multicarrier systems with blind channel estimation," *IET Communications*, pp. 2695–2704, June 2012.

[5] R. Razavi, P. Xiao, and R. Tafazolli, "Information theoretic analysis of OFDM/OQAM with utilized intrinsic interference," *IEEE Signal Processing Letters*, vol. 22, no. 5, pp. 618–622, May 2015.

[6] L. Zhang, P. Xiao, A. Zafar, A. Quddus, and R. Tafazolli, "FBMC system: An insight analysis on double dispersive channel impact," *IEEE Transactions on Vehicular Technology*, p. 10.1109/TVT.2016.2602096, to appear, 2016.

[7] I. Daubechies, "The wavelet transform, time-frequency localization and signal analysis," *IEEE Transactions on Information Theory*, vol. 36, no. 5, pp. 961–1005, Sep 1990.

[8] J. J. Benedetto, C. Heil, and D. F. Walnut, "Differentiation and the Balian-Low theorem," *J. Fourier Anal. Appl*, vol. 1, pp. 355–402, 1995.

[9] A. Sahin, I. Guvenc, and H. Arslan, "A survey on multicarrier communications: Prototype filters, lattice structures, and implementation aspects," *Communications Surveys Tutorials, IEEE*, vol. 16, no. 3, pp. 1312–1338, March 2014.

[10] M. Schellmann, Z. Zhao, H. Lin, P. Siohan, N. Rajatheva, V. Luecken, and A. Ishaque, "FBMC-based air interface for 5G mobile: Challenges and proposed solutions," *2014 9th International Conference on Cognitive Radio Oriented Wireless Networks and Communications (CROWNCOM)*, pp. 102–107, June 2014.

[11] M. Bellanger, M. Renfors, T. Ihalainen, and C. A. F. da Rocha, "OFDM and FBMC transmission techniques: A compatible high performance proposal for broadband power line communications," *Power Line Communications and Its Applications (ISPLC), 2010 IEEE International Symposium on*, pp. 154–159, March 2010.

[12] J. Yli-Kaakinen and M. Renfors, "Optimized burst truncation in fast-convolution filter bank based waveform generation," *2015 IEEE 16th International Workshop on Signal Processing Advances in Wireless Communications (SPAWC)*, pp. 71–75, June 2015.

[13] Y. Dandach and P. Siohan, "Packet transmission for overlapped offset QAM," *Wireless Communications and Signal Processing (WCSP), 2010 International Conference on*, pp. 1–6, Oct 2010.

[14] M. J. Abdoli, M. Jia, and J. Ma, "Weighted circularly convolved filtering in OFDM/OQAM," *2013 IEEE 24th Annual International Symposium on Personal, Indoor, and Mobile Radio Communications (PIMRC)*, pp. 657–661, Sept 2013.

[15] H. Lin and P. Siohan, "An advanced multi-carrier modulation for future radio systems," *2014 IEEE International Conference on Acoustics, Speech and Signal Processing (ICASSP)*, pp. 8097–8101, May 2014.

[16] H. Lin and P. Siohan, "Multi-carrier modulation analysis and WCP-COQAM proposal," *EURASIP Journal on Advances in Signal Processing*, vol. 2014, no. 1, pp. 1–19, 2014.

[17] M. Bellanger, "FS-FBMC: An alternative scheme for filter bank based multicarrier transmission," *Communications Control and Signal Processing (ISCCSP), 2012 5th International Symposium on*, pp. 1–4, May 2012.

[18] D. Mattera, M. Tanda, and M. Bellanger, "Frequency-spreading implementation of OFDM/OQAM systems," *2012 International Symposium on Wireless Communication Systems (ISWCS)*, pp. 176–180, Aug 2012.

[19] V. Berg, J. B. Doré, and D. Noguet, "A flexible FS-FBMC receiver for dynamic access in the TVWS," *2014 9th International Conference on Cognitive Radio Oriented Wireless Networks and Communications (CROWNCOM)*, pp. 285–290, June 2014.

[20] D. Mattera, M. Tanda, and M. Bellanger, "Analysis of an FBMC/OQAM scheme for asynchronous access in wireless communications," *EURASIP Journal on Advances in Signal Processing*, vol. 2015, no. 1, pp. 1–22, 2015.

[21] D. Mattera, M. Tanda, and M. Bellanger, "Frequency domain CFO compensation for FBMC systems," *Signal Processing*, vol. 114, pp. 183–197, 2015.

[22] M. Renfors, J. Yli-Kaakinen, and F. J. Harris, "Analysis and design of efficient and flexible fast-convolution based multirate filter banks," *IEEE Transactions on Signal Processing*, vol. 62, 2014.

[23] J. Yli-Kaakinen and M. Renfors, "Optimization of flexible filter banks based on fast convolution," *Journal of Signal Processing Systems*, May 2015.

[24] J. Yli-Kaakinen and M. Renfors, "Fast-convolution filter bank approach for non-contiguous spectrum use," *Future Network and Mobile Summit (FutureNetworkSummit), 2013*, pp. 1–10, July 2013.

[25] M. Renfors and J. Yli-Kaakinen, "Fast-convolution implementation of linear equalization based multiantenna detection schemes," *2014 11th International Symposium on Wireless Communications Systems (ISWCS)*, pp. 712–716, Aug 2014.

[26] M. Renfors and J. Yli-Kaakinen, "Timing offset compensation in fast-convolution filter bank based waveform processing," *Wireless Communication Systems (ISWCS 2013), Proceedings of the Tenth International Symposium on*, pp. 1–5, Aug 2013.

[27] M. Renfors and J. Yli-Kaakinen, "Channel equalization in fast-convolution filter bank based receivers for professional mobile radio," *European Wireless 2014; 20th European Wireless Conference; Proceedings of*, pp. 1–5, May 2014.

[28] K. Shao, J. Alhava, J. Yli-Kaakinen, and M. Renfors, "Fast-convolution implementation of filter bank multicarrier waveform processing," *2015 IEEE International Symposium on Circuits and Systems (ISCAS)*, pp. 978–981, May 2015.

[29] J. Javaudin, D. Lacroix, and A. Rouxel, "Pilot-aided channel estimation for OFDM/OQAM," *Vehicular Technology Conference, 2003. VTC 2003-Spring. The 57th IEEE Semiannual*, vol. 3, pp. 1581–1585 vol.3, April 2003.

[30] C. Lélé, R. Legouable, and P. Siohan, "Channel estimation with scattered pilots in OFDM/OQAM," *Signal Processing Advances in Wireless Communications, 2008. SPAWC 2008. IEEE 9th Workshop on*, pp. 286–290, July 2008.

[31] J. Bazzi, P. Weitkemper, and K. Kusume, "Power efficient scattered pilot channel estimation for FBMC/OQAM," *SCC 2015; 10th International ITG Conference on Systems, Communications and Coding; Proceedings of*, pp. 1–6, Feb 2015.

[32] C. Lélé, R. Legouable, and P. Siohan, "Iterative scattered pilot channel estimation in OFDM/OQAM," *2009 IEEE 10th Workshop on Signal Processing Advances in Wireless Communications*, pp. 176–180, June 2009.

[33] C. Lélé, "Iterative scattered-based channel estimation method for OFDM/OQAM," *EURASIP Journal on Advances in Signal Processing*, vol. 2012, no. 1, p. 42, 2012. [Online]. Available: http://dx.doi.org/10.1186/1687-6180-2012-42

[34] T. Yoon, S. Im, S. Hwang, and H. Choi, "Pilot structure for high data rate in OFDM/OQAM-IOTA system," pp. 1–5, Sept 2008.

[35] Z. Zhao, N. Vucic, and M. Schellmann, "A simplified scattered pilot for FBMC/OQAM in highly frequency selective channels," *Wireless Communications Systems (ISWCS), 2014 11th International Symposium on*, pp. 819–823, Aug 2014.

[36] X. Mestre and E. Kofidis, "Pilot-based channel estimation for FBMC/OQAM systems under strong frequency selectivity," pp. 3696–3700, March 2016.

[37] A. Viholainen, T. Ihalainen, T. H. Stitz, M. Renfors, and M. Bellanger, "Prototype filter design for filter bank based multicarrier transmission," *Signal Processing Conference, 2009 17th European*, pp. 1359–1363, Aug 2009.

[38] J. Du and S. Signell, "Time frequency localization of pulse shaping filters in OFDM/OQAM systems," *Information, Communications Signal Processing, 2007 6th International Conference on*, pp. 1–5, Dec 2007.

[39] J. G. Proakis and D. K. Manolakis, *Digital Signal Processing (4th Edition)*. Upper Saddle River, NJ, USA: Prentice-Hall, Inc., 2006.

[40] M. G. Bellanger, "Specification and design of a prototype filter for filter bank based multicarrier transmission," *2001 IEEE International Conference on Acoustics, Speech, and Signal Processing. Proceedings (Cat. No.01CH37221)*, vol. 4, pp. 2417–2420 vol.4, 2001.

[41] S. Mirabbasi and K. Martin, "Design of prototype filter for near-perfect-reconstruction overlapped complex-modulated transmultiplexers," *Circuits and Systems, 2002. ISCAS 2002. IEEE International Symposium on*, vol. 1, pp. I–821–I–824 vol.1, 2002.

[42] S. Mirabbasi and K. Martin, "Overlapped complex-modulated transmultiplexer filters with simplified design and superior stopbands," *IEEE Transactions on Circuits and Systems II: Analog and Digital Signal Processing*, vol. 50, no. 8, pp. 456–469, Aug 2003.

[43] M. Renfors and F. Harris, "Highly adjustable multirate digital filters based on fast convolution," *Circuit Theory and Design (ECCTD), 2011 20th European Conference on*, pp. 9–12, Aug 2011.

[44] D. Chen, X. G. Xia, T. Jiang, and X. Gao, "Properties and power spectral densities of CP based OQAM-OFDM systems," *IEEE Transactions on Signal Processing*, vol. 63, no. 14, pp. 3561–3575, July 2015.

[45] "Technical specification group radio access network; evolved universal terrestrial radio access (E-UTRA); physical channels and modulation, release 11," *3GPP TS 36.211 V 11.2.0*, 2013.

[46] D. Kong, D. Qu, and T. Jiang, "Time domain channel estimation for OQAM-OFDM systems: Algorithms and performance bounds," *IEEE Transactions on Signal Processing*, vol. 62, no. 2, pp. 322–330, Jan 2014.

[47] S. M. Kay, *Fundamentals of Statistical Signal Processing: Estimation Theory*. Upper Saddle River, NJ, USA: Prentice-Hall, Inc., 1993.

[48] "Technical specification group radio access network; evolved universal terrestrial radio access (E-UTRA); base station radio transmission ans reception, release 8," *3GPP TS 36.104 V 8.2.0*, 2008.